

# **Online Protein Unfolding Characterized by Ion Mobility Electron Capture Dissociation Mass Spectrometry: Cytochrome C from Neutral and Acidic Solutions**

Rebecca L. Cain<sup>1</sup>, Ian K. Webb<sup>1,2</sup> \*

<sup>1</sup>Department of Chemistry and Chemical Biology, Indiana University-Purdue University  
Indianapolis, Indianapolis, Indiana 46202, USA

<sup>2</sup>Center for Computational Biology and Bioinformatics, Indiana University School of  
Medicine, Indianapolis, Indiana 46202, USA

\*Correspondence to: Ian K. Webb; [ikwebb@iu.edu](mailto:ikwebb@iu.edu) ORCID 0000-0001-7223-8729

**Keywords:** Protein folding, ion mobility spectrometry, native mass spectrometry,  
electrospray ionization, electron capture dissociation, tandem mass spectrometry

## ABSTRACT

Electrospray ionization mass spectrometry (ESI-MS) experiments, including ion mobility-mass spectrometry (ESI-IM-MS), and electron capture dissociation (ECD) of proteins ionized from aqueous solutions, have been used for the study of solution-like structures of intact proteins. By mixing aqueous proteins with denaturants online before ESI, the amount of protein unfolding can be precisely controlled and rapidly analyzed, permitting the characterization of protein folding intermediates in protein folding pathways. Herein, we mixed various pH solutions online with aqueous cytochrome C for unfolding and characterizing its unfolding intermediates with ESI-MS charge state distribution measurements, ion mobility, and ECD. The presence of folding intermediates and unfolded cytochrome c structures were detected from changes in charge states, arrival time distributions (ATDs), and ECD fragmentation. We also compared structures from nondenaturing and denaturing solution mixtures measured under “gentle” (i.e., low energy) ion transmission conditions with structures measured under “harsh” (higher energy) transmission. This work confirms that when using “gentle” instrument conditions, the gas-phase cytochrome c ions reflect attributes of the various solution-phase structures. However, “harsh” conditions that maximize ion transmission produce annealed, extended structures that no longer correlate with changes in solution structure.

## INTRODUCTION

Mass spectrometry (MS) is a leading tool for studying protein dynamics and structure [1-4]. When studying protein function, it is important to characterize the conformational ensembles of functional, non-functional, and dysfunctional forms, gaining an understanding of what roles, primary, secondary, tertiary, and quaternary structure play in the cellular milieu [4-6]. Biophysical approaches like NMR and X-ray crystallography heavily depend on protein stability and purity while in non-native environments [7, 8], and X-ray and cryo-electron microscopy give static snapshots of protein structure [9]. Although these biophysical tools have been proven to yield incredible amounts and quality of information, mass spectrometry has unique advantages compared to other methods due to its ability to rapidly probe proteins and protein complexes as well as being able to confirm protein identity, binding, and interactions [10, 11].

Cytochrome c is a well-studied, heme-containing protein that aids in the electron transport chain [12, 13]. Cytochrome c's folding mechanism, as measured by techniques such as tryptophan fluorescence, UV circular dichroism, and hydrogen exchange [14, 15], has multiple folding phases, resulting in many different short-lived (ms time range) intermediates [16]. The first, slow step in the folding of denatured cytochrome c involves nucleation where the first several aspects of the native fold are established, followed by rapid steps involving small intermediate forms until finally refolding to its native state [15]. Methods like hydrogen exchange labeling have helped to characterize some of these folding intermediates [17]. Previous trends show that the amide groups on the N- and C-termini of folded structures are the first regions to show protection against hydrogen exchange, indicating the development of secondary structure [17]. Native (i.e., non-

denaturing) electrospray (ESI) mass spectrometry [18] has also been applied to the study of cytochrome c structure, but in the gas phase. Zhang et al. sequenced ubiquitin and cytochrome c native-like charge states from ESI from 100mM ammonium acetate solutions by electron capture dissociation (ECD) and determined that the native-like charge states fragment only in regions of higher structural dynamicity (i.e., regions with high crystallographic B factors) [19, 20] due to the tendency of ECD fragmentation to not disrupt intramolecular noncovalent bonding such as hydrogen bonding and salt bridges or fragile covalent bonds [21, 22]. Additionally, mass spectrometric studies utilizing online rapid mixing devices [23-25] have been used to control the timescales and extent of protein unfolding and refolding to study folding intermediate conformations and kinetics [24]. However, instead of changing the mixing time scale, varying the concentration of denaturant can also be used to direct protein unfolding/refolding. When paired with ion mobility (IM) and ECD, such a method of protein unfolding could give a localized picture of protein unfolding and refolding structural details.

IM and ECD paired with ESI-MS have been used to evaluate to what extent gas phase ions retain their native solution phase structures [26-30]. ESI, as a soft ionization technique, does not impart excess energy into ions as they transfer into the gas phase, allowing noncovalent interactions to be preserved [26, 31, 32]. However, there are still questions about to what extent, once in the instrument, the gas-phase ions retain native structure, especially on various instrumentation platforms that may or may not, by their nature, impart internal energy into protein ions [33]. Here we use a rapid mixing device coupled with IM and ECD for controlled protein unfolding to characterize the transfer of native-like, partially folded, and unfolded structures into the gas phase. We also

measured the IM arrival time distributions (ATDs) and ECD fragmentation patterns of ions being transferred under lower energy or higher energy conditions through the instrument to assess the effects of gas-phase activation on folded, unfolded, and intermediate structures.

## METHODS/EXPERIMENTAL

### *Reagents and materials:*

Cytochrome c from bovine heart (purchased from Sigma-Aldrich St. Louis, MO) solutions were prepared at 10 $\mu$ M in Milli-Q water (approximately pH 6.98) and stored at 20°C. Acidic solutions were made at 1, 2.5, 5, and 10 volume percent glacial acetic acid (purchased from Fischer Scientific Fairmont, NJ) in Milli-Q water corresponding to pH values 2.57, 2.35, 2.19, and 1.96, respectively, for online mixing with aqueous cytochrome c solutions.

### *Experimental Design:*

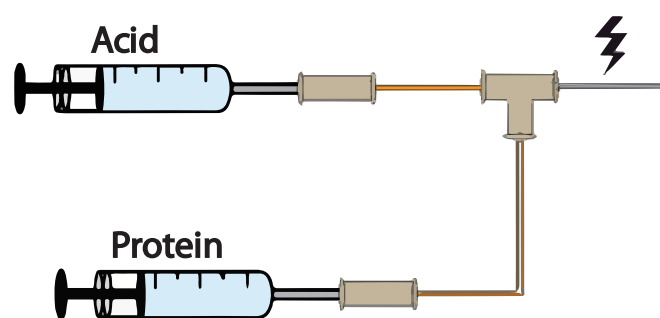


*Figure 1: Cartoon of three-way mixing tee device. Acidic solutions of various pH and cytochrome c in water are mixed online before ESI.*

The experimental arrangement was adapted from the time-resolved ESI setup developed by Konermann and coworkers [25, 34, 35]. Aqueous cytochrome c and the various acidic solutions were infused by two separate syringe pumps at 5  $\mu\text{L}/\text{min}$  into a three-way low pressure mixing tee (Idex P-714, Oak Harbor, WA) using 70 cm fused silica lines (75.5  $\mu\text{m}$  ID and 357.4  $\mu\text{m}$  OD purchased from Polymicro Technologies, Phoenix, AZ) as depicted in Figure 1. After mixing, the solution traversed a third 7 cm line pulled at the distal end with a butane torch into an emitter for ESI with an applied potential of  $\sim 3.2$  kV. The overall mixing time can be roughly estimated as 1.9 seconds (0.31  $\mu\text{L}$  volume in the third capillary). IM and mass analysis were performed with a Waters Synapt G2-Si IM-MS (Wilmslow, UK) using helium in the trap cell and He cell, nitrogen in the mobility cell, and argon in the transfer cell. To anneal cytochrome c in the gas phase to extended structures, the gas flow rates were lowered from 200 ml/min in the helium cell and 40 ml/min in the mobility cell to 25 ml/min and 7 ml/min, respectively, while keeping the traveling wave amplitude in the mobility cell the same (i.e., 40 V), dramatically increasing the ratio of the electric field to gas number density ( $E/N$ ), and thus, the ion temperatures [36]. Annealing was observed by the detection of a single narrow feature in the mobility cell suggesting an extended structure. We refer to these lower-pressure, higher  $E/N$  annealing conditions as “harsh” conditions and the higher-pressure, lower  $E/N$  conditions as “gentle” conditions. Under each different condition, each cytochrome c charge state was  $m/z$  selected before mobility separation and then subjected to ECD (eMSion Corvallis, OR) after mobility selection. ECD settings were optimized for maximum electron capture and minimum collisional heating. In the ECD cell, we observed that increasing the LM5 voltage decreases collisional heating, observed by the elimination of the protonated heme peak

presumably produced by collision induced dissociation (CID). Therefore, we increased the voltage difference between the LM5 and L6 lenses in the ECD cell to slow the gas ions. The ECD settings were also optimized for each different instrument setting. Under gentle conditions, the ECD lenses used much lower voltages of L1 0.0, L2 10.0, LM3 3.0, L4 7.0, FB 3.5, LM5 5.0, L6 15.0, L7 15.0, while harsh instrument conditions used lens voltages of L1 -23.3, L2 -17.0, LM3 -0.4, FB 8.6, LM5 13.0, L6 27, L7 27.

*Data analysis:*

ECD data for each charge state under each different condition were collected in triplicate. After fragmentation, c and z ions were annotated by LCMS Spectator using a 20 ppm mass error [37] and then manually verified for each replicate. Fragments observed in less than two spectra were not counted. The filtered sequence fragments for each charge state under each condition were visualized in Prosight Lite [38].

## RESULTS AND DISCUSSION

### *Charge State Distributions*

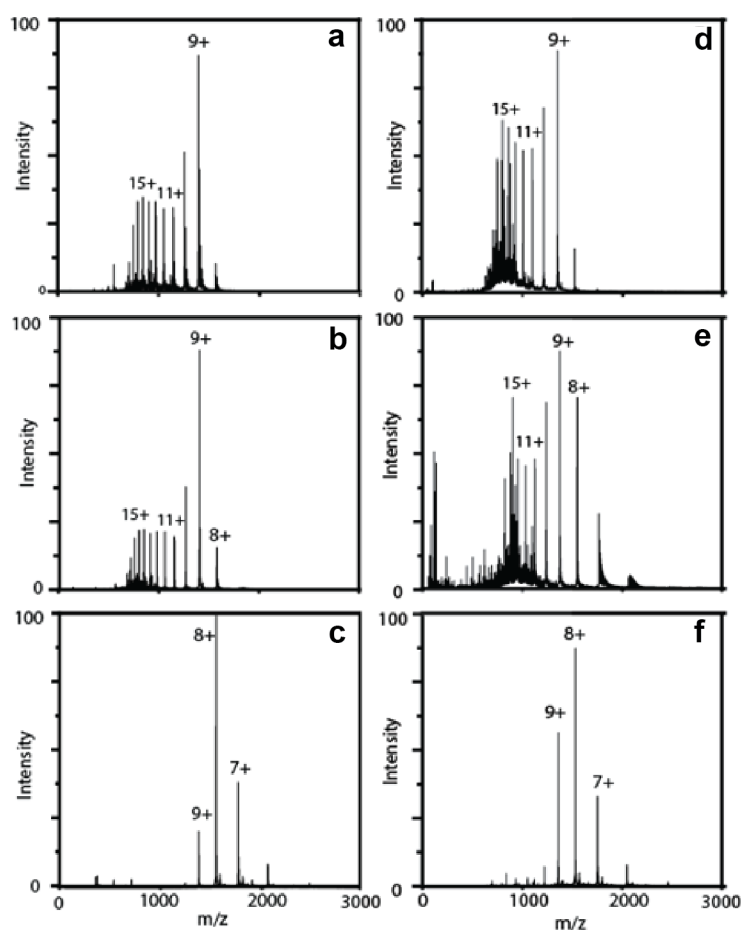


*Figure 2: Full ESI mass spectra for cytochrome c under gentle conditions upon mixing with 10% acetic acid (a), 5% acetic acid (b), and water (c) and under harsh conditions mixing with 10% acetic acid (d), 5% acetic acid (e), and water (f).*

The ESI spectrum of cytochrome c from neutral (pH 6.98) water, for both harsh and gentle instrument conditions, displayed low charge states; 6<sup>+</sup>, 7<sup>+</sup>, 8<sup>+</sup>, and 9<sup>+</sup> (Figure 2c, f). Folded protein conformations have fewer accessible sites for protonation by ESI, so these conformations are represented by the lowest charge states [39]. Therefore, the



charge states from ESI of cytochrome c under neutral solution conditions correlate with compact, folded protein conformations. As expected, the observed charge state distribution was not dramatically changed between harsh and gentle instrument conditions since these are post-ionization changes. However, the signal-to-noise ratio was noticeably lower for the gentler ion transmission settings, as is typically observed when trying to reduce ion heating [40]. When the acidity of the mixing solution was 5% acetic acid (pH 2.19, pH of post-mixing water/acidic solution roughly 2.35), under both gentle and harsh instrument conditions, the charge state distribution shifts to include higher charge states of 10-18<sup>+</sup> (Figure 2 b and e). In these low pH conditions, a greater number of basic residues are available for protonation due to unfolding, resulting in higher charge states [41]. The lowest charge states, 6<sup>+</sup> and 7<sup>+</sup>, substantially decrease, correlating with a decrease in the abundance of the native state. However, the presence of the abundant 9<sup>+</sup> charge state indicates that a dominant compact species, though possibly a different structure than the native state, is present with the unfolded state. This specific bimodal distribution reflects a transition from the native state into at least two states, one more extended than the other, which correlates with other methods, such as Soret absorption, fluorescence, circular dichroism, and small angle X-ray scattering [42], as well as other ESI measurements of charge state distribution changes upon decreasing pH [34, 43]. These other measurements show that the populations of acid-induced unfolded and molten globular (i.e., compact, non-native) structures are maximized at approximately pH 2. It is also apparent that the higher E/N of the harsher conditions results in significant CID of the highest charge states, evidenced by the reduction in the signal of the highest charge states and the appearance of many additional peaks that are

not precursor ion charge states. The most acidic condition, 10% acetic acid (pH 1.96, pH of post-mixing water/acidic solution roughly 2.19) under both gentle and harsh conditions, shows a similar charge state distribution (Figures 2 a and d). However, the most abundant charge state shifts from the 9<sup>+</sup> charge state to the 10<sup>+</sup> charge state under the lower pressure conditions and the 15<sup>+</sup> charge state in the higher-pressure condition, evidence of a shift in the overall population of solution structures to more unfolded structures. The differences in the harsh and gentle spectra with 10% acetic acid are again attributed to additional ion heating and CID at higher E/N. Mixing the protein with 1% and 2.5% acetic acid (pH 2.57 and 2.35, respectively, with pH of post-mixing water/acidic solution roughly 2.87 and 2.57), did not show major shifts in the charge state distribution. Therefore, experiments run in water and mixed with 5%, and 10% acetic acid are the only ones discussed in this work. We refer to the mixtures of the aqueous protein with 5% and 10% acid via the mixing tee by their final mixed pH values throughout the remainder of the text.

## *Ion Mobility*

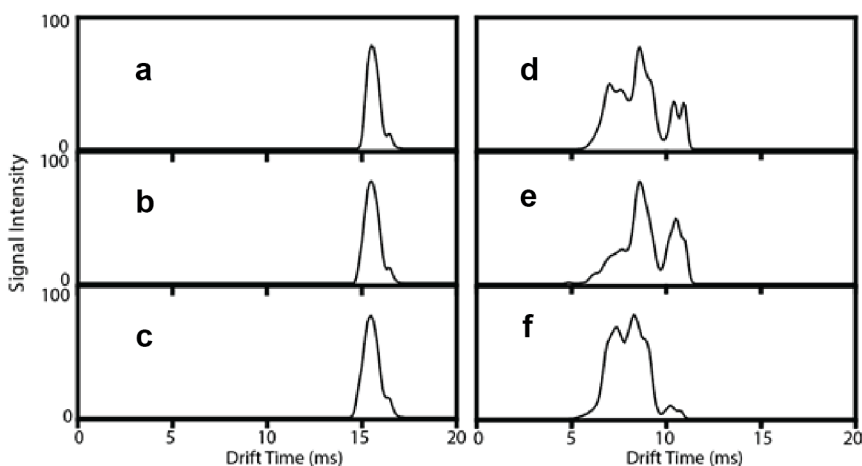


*Figure 3: Ion mobility spectra for cytochrome c 9+ under harsh conditions at pH 2.19 (a), pH 2.35 (b), and water (c) and under gentle conditions at pH 2.19 (d), pH 2.35 (e), and water (f).*

The ATDs of proteins represent the overall shape/size of kinetically trapped, ion conformations if care is used to minimize collisional or thermal activation [4]. The various peaks in ATDs correlate with the different conformations present. Multiple broad, unresolved features indicate many conformations while narrow peaks indicate only one conformational family. Cytochrome c 9<sup>+</sup> is present in each solution and instrumental condition tested and thus can be used as a representative charge state for probing the effects of acid-induced unfolding on IM ATDs. Under gentle conditions, the ion mobility peaks for each acidic condition tested show broad peaks representing multiple conformations. Since the 9<sup>+</sup> charge state is one of the most abundant charge states for each solution condition, it is expected to show evidence of molten globular [43] or other intermediate states in equilibrium with the most compact states. For example, in Figure 3, the mobility spectra for cytochrome c 9<sup>+</sup> in water (f) show multiple broad features.

However, the mobility peaks for pH 2.35 and pH 2.19 (e and d) have more abundant extended features (above 10 ms), due to the increase in more extended states. The many  $9^+$  features correlate with solution measurements of cytochrome c refolding having multiple folding intermediates [44]. Under the harsh instrument conditions, the mobility peaks in Figure 3 a, b, and c mobility spectra for the  $9^+$  charge state are all narrow peaks, showing only one major feature with a small shoulder. The narrow peaks for each of the solution conditions correlate with the harsh instrument conditions resulting in the annealing of the protein to fewer conformations. Since the ATDs from the different solution conditions are virtually identical under harsh conditions, they likely cannot inform on the solution distribution of structures.

The other charge states of cytochrome c also show similar trends in their ion mobility spectra. The  $7^+$  charge state under gentle conditions has a single broad mobility peak when electrosprayed from neutral pH, indicating this lower charge state presents an ensemble of compact states in the gas phase (Figure S-1 a). Cytochrome c  $8^+$  ionized from pure water results in a similar ATD to the  $7^+$  under gentle conditions (Figure S-1 b). When the pH is reduced to 2.35, the  $8^+$  ions shift mostly to more extended distributions, showing unfolding behavior (Figure S-1 c). At pH 2.19, the ATD shows a high intensity, broad peak at  $\sim 7.72$  ms (Figure S-1 d), indicating that a significant portion of the cytochrome c population refolds, likely into the molten globular state. Higher charge states ( $11^+$  and  $15^+$ ) are only observed at pH 2.35 and pH 2.19. These charge states lead to narrower distributions under both solution conditions (Figure S-1 e-h), indicative of extended cytochrome c structures. Overall, these ATDs are in excellent agreement with

ATDs measured with similar instrumentation for acid-induced cytochrome c unfolding [25].

Under harsh conditions for each different acidic condition, the other charge states (e.g., 7<sup>+</sup>, 8<sup>+</sup>, 11<sup>+</sup>, Figure S-2) all have singular, narrow peaks, following the trend of the 9<sup>+</sup>. This means that each of the cytochrome c charge states is annealed to more extended structures under harsh instrument conditions. These gas-phase conformers, as represented by their ATDs, no longer correlate with the ionization solution pH. The presence of singular, narrow peaks for gas-phase annealed cytochrome c ions agrees with the ATDs at the highest collisional energies for other examples of the gas-phase annealing of cytochrome c ions in the literature [45, 46].

### *ECD Under gentle Conditions*

#### **a** 10% sequence coverage

```

N  G D V E K G K K I F V Q K C A Q C H T V E K G G K 25
26  H K T G P N L H G L F G R K T G Q A P G F T Y T D 50
51  A N K N K G I T W K E E T L M E Y L E N P K K Y I 75
76  P G T K M I F A G I K K K T E R E D L I A Y L K K 100
101 A T N E C

```

#### **b** 15% sequence coverage

```

N  G D V E K G K K I F V Q K C A Q C H T V E K G G K 25
26  H K T G P N L H G L F G R K T G Q A P G F T Y T D 50
51  A N K N K G I T W K E E T L M E Y L E N P K K Y I 75
76  P G T K M I F A G I K K K T E R E D L I A Y L K K 100
101 A T N E C

```

#### **c** 35% sequence coverage

```

N  G D V E K G K K I F V Q K C A Q C H T V E K G G K 25
26  H K T G P N L H G L F G R K T G Q A P G F T Y T D 50
51  A N K N K G I T W K E E T L M E Y L E N P K K Y I 75
76  P G T K M I F A G I K K K T E R E D L I A Y L K K 100
101 A T N E C

```

*Figure 4: ECD sequence coverage of cytochrome c 9<sup>+</sup> under gentle instrument conditions in water (a), pH 2.35 (b), and pH 2.19 (c).*

While the ion mobility ATDs reflect the overall gas-phase structures of cytochrome c, ECD fragmentation is used as a higher structural resolution, albeit indirect, measurement of the changes in cytochrome c structure. Regional increases in fragmentation are suggestive of unfolding and refolding into structures that have lost native contacts in these areas. The cytochrome c heme is covalently bound to cysteines 14 and 17, and the heme iron is bound to methionine 80 [13, 47]. Therefore, we expect that natively folded cytochrome c structures would show limited fragmentation between cysteine 14 and methionine 80, since even if the protein backbone is fragmented by ECD, the bonds to the heme and iron bind fragments in this region together, preventing the detection of fragment ions by their unique  $m/z$ . Under gentle instrument conditions, the 9<sup>+</sup> charge state shows ECD fragmentation almost exclusively N-terminal to cysteine 14 and C-terminal to methionine 80, correlating with a structure similar to the natively folded solution structure (Figure 4). However, ECD sequence coverage increases from 10% sequence coverage to 35% as the acidity increases from water to pH 2.19. Figure 4 b (pH 2.35) shows several fragments between cysteine 14 and methionine 80, whereas Figure 4 c (pH 2.19) shows extensive fragmentation throughout the protein. These results correlate with the loss of the methionine 80/iron ligand bond dissociation upon the addition of acid, supporting evidence from fluorescence spectroscopy that the acidified cytochrome c loses the iron to methionine 80 bond [15]. The increase in sequence coverage from pH 2.35 to pH 2.19 indicates the loss of additional salt bridges, hydrogen bonds, or other intramolecular interactions with the additional decrease in pH. Specifically, there is

extensive fragmentation observed between lysine 79 and aspartic acid 93. These residues do not directly interact in the cytochrome c crystal structure as they are distant from each other [48]. This likely indicates that this putative salt bridge [49] that is disrupted between pH 2.35 and pH 2.19 is a new intramolecular bond formed after unfolding and refolding into an intermediate structure upon mixing with the pH 2.35 acid solution. Similarly, there is a marked increase in fragmentation for pH 2.19 versus pH 2.35 between lysine 53 and glutamic acid 69. These residues are much closer in the crystal structure. Further examination reveals that the lysine side chain is hydrogen bound to the backbone carbonyl oxygen of tyrosine 74 under native conditions. Therefore, it is likely that this intramolecular bond may be preserved at pH 2.35 but is lost upon acidifying to the pH 2.19 condition, allowing observation of fragments in this region.

The lower charge states in water, such as the 7<sup>+</sup> charge state, had ATDs that showed evidence of compact gas-phase structures, which we expect would correlate with the retention of an increased number of native contacts. The ECD sequence coverage of 14% from the 7<sup>+</sup> charge state, also covering only from the N-terminal to cysteine 14 and C-terminal to methionine 80 (Figure S-3), correlates to many stabilizing intramolecular interactions, similarly to what was observed for 9<sup>+</sup>. The most dominant charge state when electrosprayed from water, 8<sup>+</sup>, has a sequence coverage of 23% with fragmentation focused around both termini (Figure S-4). The terminal regions of the protein have the highest B-factor in the crystal structure (i.e., the most flexible regions) and are expected to fragment readily even for the native structure [19]. As the acidity, and therefore protein unfolding, increases, the 7<sup>+</sup> charge state is no longer present and the 8<sup>+</sup> charge state abundance decreases so significantly that ECD fragments are no longer detectable above

the noise baseline. As the protein intramolecular bonds are disrupted more to produce unfolded higher charge states, the ECD fragmentation expands from just the N-terminal and C-terminal fragments again between cysteine 14 and 80. Following the trends of the 9<sup>+</sup>, the higher charge states such as 11<sup>+</sup> and 15<sup>+</sup> have extensive fragmentation in the interior region of the protein (Figure S-5 and S-6). At pH 2.35 and pH 2.19, cytochrome c 15<sup>+</sup> has ECD sequence coverage of 44% and 54%, respectively, with fragments throughout the protein, reflecting a trend of increasing ECD coverage as the acidity increases and the protein unfolds. As the protein unfolds in acetic acid, the higher charge states increased ECD sequence coverage correlates with the loss of native contacts and iron to methionine 80 binding.

### *ECD Under Harsh Conditions*

#### **a 58% sequence coverage**

**N** G D V E **K** **G** **K** **K** I F V Q K **C** A Q C H T V E **K** **G** **G** **K** 25  
 26 H K T **G** P **N** L H **G** **L** F **G** **R** **K** T **G** **Q** A P **G** **F** **T** **Y** **T** **D** 50  
 51 **A** **N** **K** **N** **K** **G** I T W **K** **E** **E** T L M **E** **Y** **L** **E** **N** P **K** **K** **Y** I 75  
 76 P **G** **T** **K** M I F **A** **G** **I** **K** **K** **K** T **E** **R** **E** **D** L I **A** **Y** **L** **K** **K** 100  
 101 **A** T N E C

#### **b 72% sequence coverage**

**N** G D V E **K** **G** **K** **K** I F V Q K **C** A Q C H T V E **K** **G** **G** **K** 25  
 26 H **K** T **G** P **N** L H **G** **L** F **G** **R** **K** T **G** **Q** A P **G** **F** **T** **Y** **T** **D** 50  
 51 **A** **N** **K** **N** **K** **G** I T W **K** **E** **E** T L M **E** **Y** **L** **E** **N** P **K** **K** **Y** I 75  
 76 P **G** **T** **K** M I F **A** **G** **I** **K** **K** **K** T **E** **R** **E** **D** L I **A** **Y** **L** **K** **K** 100  
 101 A T N E C

#### **c 72% sequence coverage**

**N** G D V E **K** **G** **K** **K** I F V Q K **C** A Q C H T V E **K** **G** **G** **K** 25  
 26 H **K** T **G** P **N** L H **G** **L** F **G** **R** **K** T **G** **Q** A P **G** **F** **T** **Y** **T** **D** 50  
 51 **A** **N** **K** **N** **K** **G** I T W **K** **E** **E** T L M **E** **Y** **L** **E** **N** P **K** **K** **Y** I 75  
 76 P **G** **T** **K** M I F **A** **G** **I** **K** **K** **K** T **E** **R** **E** **D** L I **A** **Y** **L** **K** **K** 100  
 101 A T N E C

*Figure 5: ECD sequence coverage of cytochrome c 9<sup>+</sup> under harsh instrument conditions in water (a), pH 2.35 (b), and pH 2.19 (c).*



When the instrument is operated under lower pressure/harsh conditions, similar to the gentle conditions, there is an increased sequence coverage as the acidity of the denaturing conditions increases. However, for the 9<sup>+</sup> charge state, all solution conditions analyzed under harsh parameters exhibit much more fragmentation than any of the solution states fragmented by ECD with gentle instrument conditions. This is likely due to the elimination of intramolecular interactions due to extensive ion heating [50], which was also observed for the ATDs under these harsh conditions. Cytochrome c 9<sup>+</sup> ECD sequence coverage increases from 54% in water to 72% at pH 2.35 and pH 2.19 as the ion heating further unfolds the protein compared to only solution unfolding before analysis with ion transmission under gentle conditions (10%, 15%, and 35% respectively). Instead of exclusively fragmenting from the N-terminus to cysteine 14 and C-terminus to methionine 80 in the pH 6.98 mixtures, ECD fragmentation occurs throughout the protein. This correlates with the ion heating under the harsh instrument conditions resulting in structures that do not closely resemble solution structures since all three solvent conditions show extensive fragmentation. The 11<sup>+</sup> charge state has ECD sequence coverage that is virtually identical in both acidic conditions, from 66% at pH 2.35 to 68% at pH 2.19 (Figure S-5). The fragmentation under harsh conditions for the lower charge states also does not follow the same fragmentation patterns as under gentle conditions. The more folded 7<sup>+</sup> and 8<sup>+</sup> charge states in water both show sequence coverage of 57% in neutral solutions (Figure S-3 and S-4). However, the 15<sup>+</sup> charge state was not transferred through the instrument in high enough abundance to observe under harsh conditions.

## CONCLUSION

The combination of online mixing with ion mobility and ECD was used to identify the structural details of steps in the protein folding process. By decreasing the ESI pH, the charge state distribution for cytochrome c shifted to higher charge states that indicate the presence of more extended structures. Ion mobility spectra of the various charge states under gentle instrument conditions showed evidence for multiple protein conformations in their ATDs. For the lowest charge states, broad peaks correlated to the coexistence of several compact, native-like states when ionized from water, but additional, more extended features were observed upon acidification. The 9<sup>+</sup> ions, having intermediate charge, as well as the highest charge states, resulted in multiple peaks at various levels of acidification indicating various stages of protein unfolding/refolding. While using harsh instrument conditions, ion mobility spectra contain singular narrow peaks due to the proteins annealing in the gas phase into more extended conformers by collisional activation.

ECD fragmentation of the various charge states of cytochrome c reflected differences in structure induced by acidification. The charge states observed from pure water showed fragmentation only at the flexible termini of the proteins but not within the interior of the protein, bound together by intramolecular interactions and from binding to the iron by methionine 80 and the heme by cysteine 14 and 16. Upon acidification, ECD fragmentation reflected the loss of the iron-methionine 80 bond as well as other native and non-native contacts. However, under harsh conditions, fragmentation was drastically different, showing extensive sequence coverage for all charge states regardless of the ESI solution pH.

Several important conclusions can be drawn from these studies. First, the structures probed by IM/MS under gentle conditions are not equilibrium gas-phase structures, as neither the ATDs nor ECD fragments from harsh conditions reflect the unfolded/refolded protein ions examined under gentle conditions. Therefore, these experiments demonstrate the utility of native IM/MS methods for characterizing protein folding intermediates under the timescale of the IM measurement. Second, we note that our unfolding measurements, along with the measurements of others, show that tuning mass spectrometry conditions for maximum transmission leads to the unfolding of the protein in the gas phase into structures that likely have little biological relevance. Thus, echoing the work of others, we recommend that special care be given to the parameters used to study the protein unfolding and other dynamics by native IM/MS methods.

#### ACKNOWLEDGEMENTS

Portions of this work were funded by National Science Foundation CAREER CHE-2143755. The authors would like to acknowledge Professor Derek Wilson and his research group for helpful discussions.

#### CONFLICT OF INTEREST STATEMENT

The authors have no conflicts of interest to declare.

## REFERENCES

1. Lossel, P; van de Waterbeemd, M; Heck, AJ. The diverse and expanding role of mass spectrometry in structural and molecular biology. *EMBO J.* 2016;35:2634-57. <https://doi.org/10.15252/embj.201694818>
2. Hodge, EA; Benhaim, MA; Lee, KK. Bridging protein structure, dynamics, and function using hydrogen/deuterium-exchange mass spectrometry. *Protein Sci.* 2020;29:843-55. <https://doi.org/10.1002/pro.3790>
3. Sinz, A; Arlt, C; Chorev, D; Sharon, M. Chemical cross-linking and native mass spectrometry: A fruitful combination for structural biology. *Protein Sci.* 2015;24:1193-209. <https://doi.org/10.1002/pro.2696>
4. Clemmer, DE; Russell, DH; Williams, ER. Characterizing the Conformationome: Toward a Structural Understanding of the Proteome. *Acc. Chem. Res.* 2017;50:556-60. <https://doi.org/10.1021/acs.accounts.6b00548>
5. Dill, KA; MacCallum, JL. The protein-folding problem, 50 years on. *Science.* 2012;338:1042-6. <https://doi.org/10.1126/science.1219021>
6. Shen, H-B; Chou, K-C. QuatIdent: A Web Server for Identifying Protein Quaternary Structural Attribute by Fusing Functional Domain and Sequential Evolution Information. *J. Proteome Res.* 2009;8:1577-84. <https://doi.org/10.1021/pr800957q>
7. Chavez, JD; Bruce, JE. Chemical cross-linking with mass spectrometry: a tool for systems structural biology. *Curr. Opin. Chem. Biol.* 2019;48:8-18. <https://doi.org/10.1016/j.cbpa.2018.08.006>
8. Yee, AA; Savchenko, A; Ignachenko, A; Lukin, J; Xu, X; Skarina, T; Evdokimova, E; Liu, CS; Semesi, A; Guido, V; et al. NMR and X-ray crystallography, complementary tools in structural proteomics of small proteins. *J. Am. Chem. Soc.* 2005;127:16512-7. <https://doi.org/10.1021/ja053565+>
9. Wells, JN; Marsh, JA. Experimental Characterization of Protein Complex Structure, Dynamics, and Assembly. In: Marsh, J. A., editors. *Protein Complex Assembly: Methods and Protocols.* New York, NY:Springer New York; 2018. pp 3-27.
10. Kaltashov, IA; Eyles, SJ. Studies of biomolecular conformations and conformational dynamics by mass spectrometry. *Mass Spectrom. Rev.* 2002;21:37-71. <https://doi.org/10.1002/mas.10017>
11. Smith, DP; Giles, K; Bateman, RH; Radford, SE; Ashcroft, AE. Monitoring copopulated conformational states during protein folding events using electrospray ionization-ion mobility spectrometry-mass spectrometry. *J. Am. Soc. Mass Spectrom.* 2007;18:2180-90. <https://doi.org/10.1016/j.jasms.2007.09.017>
12. Ow, Y-LP; Green, DR; Hao, Z; Mak, TW. Cytochrome c: functions beyond respiration. *Nat. Rev. Mol. Cell Biol.* 2008;9:532-42. <https://doi.org/10.1038/nrm2434>
13. Stevens, JM; Mavridou, DA; Hamer, R; Kritsiligkou, P; Goddard, AD; Ferguson, SJ. Cytochrome c biogenesis System I. *FEBS J.* 2011;278:4170-8. <https://doi.org/10.1111/j.1742-4658.2011.08376.x>
14. Colón, W; Elöve, GA; Wakem, LP; Sherman, F; Roder, H. Side Chain Packing of the N- and C-Terminal Helices Plays a Critical Role in the Kinetics of Cytochrome c Folding. *Biochemistry.* 1996;35:5538-49. <https://doi.org/10.1021/bi960052u>
15. Englander, SW; Sosnick, TR; Mayne, LC; Shtilerman, M; Qi, PX; Bai, Y. Fast and Slow Folding in Cytochrome c. *Acc. Chem. Res.* 1998;31:737-44. <https://doi.org/10.1021/ar970085h>

16. Travaglini-Allocatelli, C; Gianni, S; Brunori, M. A common folding mechanism in the cytochrome c family. *Trends Biochem Sci* 2004;29:535-41.  
<https://doi.org/10.1016/j.tibs.2004.08.004>
17. Roder, H; Elove, GA; Englander, SW. Structural characterization of folding intermediates in cytochrome c by H-exchange labelling and proton NMR. *Nature*. 1988;335:700-4. <https://doi.org/10.1038/335700a0>
18. Leney, AC; Heck, AJR. Native Mass Spectrometry: What is in the Name? *J. Am. Soc. Mass Spectrom.* 2017;28:5-13. <https://doi.org/10.1007/s13361-016-1545-3>
19. Zhang, H; Cui, W; Gross, ML. Native electrospray ionization and electron-capture dissociation for comparison of protein structure in solution and the gas phase. *Int. J. Mass Spectrom.* 2013;354-355:10.1016/j.ijms.2013.06.019.  
<https://doi.org/10.1016/j.ijms.2013.06.019>
20. Fenn, LS; Kliman, M; Mahsut, A; Zhao, SR; McLean, JA. Characterizing ion mobility-mass spectrometry conformation space for the analysis of complex biological samples. *Anal Bioanal Chem* 2009;394:235-44. <https://doi.org/10.1007/s00216-009-2666-3>
21. Zubarev, RA; Kelleher, NL; McLafferty, FW. Electron capture dissociation of multiply charged protein cations. A nonergodic process. *J. Am. Chem. Soc.* 1998;120:3265-6. [https://doi.org/DOI 10.1021/ja973478k](https://doi.org/DOI%2010.1021/ja973478k)
22. Breuker, K; Oh, H; Lin, C; Carpenter, BK; McLafferty, FW. Nonergodic and conformational control of the electron capture dissociation of protein cations. *Proc. Natl. Acad. Sci. U.S.A.* 2004;101:14011-6. <https://doi.org/10.1073/pnas.0406095101>
23. Wilson, DJ; Konermann, L. A capillary mixer with adjustable reaction chamber volume for millisecond time-resolved studies by electrospray mass spectrometry. *Anal. Chem.* 2003;75:6408-14. <https://doi.org/10.1021/ac0346757>
24. Zinck, N; Stark, AK; Wilson, DJ; Sharon, M. An improved rapid mixing device for time-resolved electrospray mass spectrometry measurements. *Chemistryopen*. 2014;3:109-14. <https://doi.org/10.1002/open.201402002>
25. Liuni, P; Deng, B; Wilson, DJ. Comparing equilibrium and kinetic protein unfolding using time-resolved electrospray-coupled ion mobility mass spectrometry. *Analyst*. 2015;140:6973-9. <https://doi.org/10.1039/C5AN00843C>
26. Wyttenbach, T; Bowers, MT. Structural stability from solution to the gas phase: native solution structure of ubiquitin survives analysis in a solvent-free ion mobility-mass spectrometry environment. *J. Phys. Chem. B.* 2011;115:12266-75.  
<https://doi.org/10.1021/jp206867a>
27. Breuker, K; Oh, H; Horn, DM; Cerda, BA; McLafferty, FW. Detailed unfolding and folding of gaseous ubiquitin ions characterized by electron capture dissociation. *J. Am. Chem. Soc.* 2002;124:6407-20. <https://doi.org/10.1021/ja012267j>
28. Skinner, OS; McLafferty, FW; Breuker, K. How ubiquitin unfolds after transfer into the gas phase. *J. Am. Soc. Mass Spectrom.* 2012;23:1011-4.  
<https://doi.org/10.1007/s13361-012-0370-6>
29. Ruotolo, BT; Giles, K; Campuzano, I; Sandercock, AM; Bateman, RH; Robinson, CV. Evidence for macromolecular protein rings in the absence of bulk water. *Science*. 2005;310:1658-61. <https://doi.org/10.1126/science.1120177>
30. Ruotolo, BT; Robinson, CV. Aspects of native proteins are retained in vacuum. *Curr. Opin. Chem. Biol.* 2006;10:402-8. <https://doi.org/10.1016/j.cbpa.2006.08.020>

31. Robinson, CV; Chung, EW; Kragelund, BB; Knudsen, J; Aplin, RT; Poulsen, FM; Dobson, CM. Probing the nature of noncovalent interactions by mass spectrometry. A study of protein-CoA ligand binding and assembly. *J. Am. Chem. Soc.* 1996;118:8646-53. <https://doi.org/10.1021/ja960211x>
32. Seo, J; Hoffmann, W; Warnke, S; Bowers, MT; Pagel, K; von Helden, G. Retention of Native Protein Structures in the Absence of Solvent: A Coupled Ion Mobility and Spectroscopic Study. *Angew. Chem. Int. Ed.* 2016;55:14173-6. <https://doi.org/10.1002/anie.201606029>
33. Merenbloom, SI; Flick, TG; Williams, ER. How Hot are Your Ions in TWAVE Ion Mobility Spectrometry? *J. Am. Soc. Mass Spectrom.* 2012;23:553-62.
34. Konermann, L; Collings, BA; Douglas, DJ. Cytochrome c Folding Kinetics Studied by Time-Resolved Electrospray Ionization Mass Spectrometry. *Biochemistry.* 1997;36:5554-9. <https://doi.org/10.1021/bi970046d>
35. Konermann, L; Pan, J; Wilson, DJ. Protein folding mechanisms studied by time-resolved electrospray mass spectrometry. *Biotechniques.* 2006;40:135-41. <https://doi.org/10.2144/06402te01>
36. Revercomb, HE; Mason, EA. Theory of plasma chromatography/gaseous electrophoresis. Review. *Anal. Chem.* 1975;47:970-83. <https://doi.org/10.1021/ac60357a043>
37. Park, J; Piehowski, PD; Wilkins, C; Zhou, M; Mendoza, J; Fujimoto, GM; Gibbons, BC; Shaw, JB; Shen, Y; Shukla, AK; et al. Informed-Proteomics: open-source software package for top-down proteomics. *Nat. Methods.* 2017;14:909-14. <https://doi.org/10.1038/nmeth.4388>
38. Fellers, RT; Greer, JB; Early, BP; Yu, X; LeDuc, RD; Kelleher, NL; Thomas, PM. ProSight Lite: graphical software to analyze top-down mass spectrometry data. *Proteomics.* 2015;15:1235-8. <https://doi.org/10.1002/pmic.201570050>
39. Kaltashov, IA; Mohimen, A. Estimates of Protein Surface Areas in Solution by Electrospray Ionization Mass Spectrometry. *Anal. Chem.* 2005;77:5370-9. <https://doi.org/10.1021/ac050511>
40. Chen, S-H; Russell, DH. How Closely Related Are Conformations of Protein Ions Sampled by IM-MS to Native Solution Structures? *J. Am. Soc. Mass Spectrom.* 2015;26:1433-43. <https://doi.org/10.1007/s13361-015-1191-1>
41. Konermann, L; Douglas, DJ. Acid-Induced Unfolding of Cytochrome c at Different Methanol Concentrations: Electrospray Ionization Mass Spectrometry Specifically Monitors Changes in the Tertiary Structure. *Biochemistry.* 1997;36:12296-302. <https://doi.org/10.1021/bi971266u>
42. Goto, Y; Hagihara, Y; Hamada, D; Hoshino, M; Nishii, I. Acid-induced unfolding and refolding transitions of cytochrome c: A three-state mechanism in water and deuterium oxide. *Biochemistry.* 1993;32:11878-85. <https://doi.org/10.1021/bi00095a017>
43. Rob, T; Wilson, DJ. A versatile microfluidic chip for millisecond time-scale kinetic studies by electrospray mass spectrometry. *J. Am. Soc. Mass Spectrom.* 2009;20:124-30. <https://doi.org/10.1016/j.jasms.2008.09.005>
44. Winkler, JR. Cytochrome c folding dynamics. *Curr. Opin. Chem. Biol.* 2004;8:169-74. <https://doi.org/https://doi.org/10.1016/j.cbpa.2004.02.009>

45. Yin, V; Konermann, L. Probing the Effects of Heterogeneous Oxidative Modifications on the Stability of Cytochrome c in Solution and in the Gas Phase. *J. Am. Soc. Mass Spectrom.* 2021;32:73-83. <https://doi.org/10.1021/jasms.0c00089>
46. Borotto, NB; Osho, KE; Richards, TK; Graham, KA. Collision-Induced Unfolding of Native-like Protein Ions Within a Trapped Ion Mobility Spectrometry Device. *J. Am. Soc. Mass Spectrom.* 2022;33:83-9. <https://doi.org/10.1021/jasms.1c00273>
47. Fisher, WR; Taniuchi, H; Anfinsen, CB. On the role of heme in the formation of the structure of cytochrome c. *J. Biol. Chem.* 1973;248:3188-95. [https://doi.org/10.1016/S0021-9258\(19\)44026-X](https://doi.org/10.1016/S0021-9258(19)44026-X)
48. Bushnell, GW; Louie, GV; Brayer, GD. High-resolution three-dimensional structure of horse heart cytochrome c. *J. Mol. Biol.* 1990;214:585-95. [https://doi.org/10.1016/0022-2836\(90\)90200-6](https://doi.org/10.1016/0022-2836(90)90200-6)
49. Zhang, Z; Vachet, RW. Gas-Phase Protein Salt Bridge Stabilities from Collisional Activation and Electron Transfer Dissociation. *Int. J. Mass Spectrom.* 2017;420:51-6. <https://doi.org/10.1016/j.ijms.2016.09.010>
50. Molano-Arevalo, JC; Jeanne Dit Fouque, K; Pham, K; Miksovská, J; Ridgeway, ME; Park, MA; Fernandez-Lima, F. Characterization of Intramolecular Interactions of Cytochrome c Using Hydrogen-Deuterium Exchange-Trapped Ion Mobility Spectrometry-Mass Spectrometry and Molecular Dynamics. *Anal. Chem.* 2017;89:8757-65. <https://doi.org/10.1021/acs.analchem.7b00844>